

# Coded DS-CDMA Systems with Iterative Channel Estimation and no Pilot Symbols

Don Torrieri, *Senior Member, IEEE*, Amitav Mukherjee, *Student Member, IEEE*,  
and Hyuck M. Kwon, *Senior Member, IEEE*

## Abstract

In this paper, we describe direct-sequence code-division multiple-access (DS-CDMA) systems with quadriphase-shift keying in which channel estimation, coherent demodulation, and decoding are iteratively performed without the use of any training or pilot symbols. An expectation-maximization channel-estimation algorithm for the fading amplitude, phase, and the interference power spectral density (PSD) due to the combined interference and thermal noise is proposed for DS-CDMA systems with irregular repeat-accumulate codes. After initial estimates of the fading amplitude, phase, and interference PSD are obtained from the received symbols, subsequent values of these parameters are iteratively updated by using the soft feedback from the channel decoder. The updated estimates are combined with the received symbols and iteratively passed to the decoder. The elimination of pilot symbols simplifies the system design and allows either an enhanced information throughput, an improved bit error rate, or greater spectral efficiency. The interference-PSD estimation enables DS-CDMA systems to significantly suppress interference.

## Index Terms

Code-division multiple access (CDMA), channel estimation, pilot symbols, expectation-maximization algorithm, iterative receiver.

## I. INTRODUCTION

In mobile communication systems, the wireless channel induces random amplitude and phase variations in the received data, with the possible addition of time-varying interference from co-channel users. For this reason, the accuracy of channel state information (CSI) at the receiver is critical for coherent detection and demodulation. A number of methods have been proposed for estimation of CSI, all of which fall within the broad categories of either pilot-assisted or blind algorithms. Current and next-generation cellular protocols such as W-CDMA (Wideband Code Division Multiple Access) and 3GPP LTE (Third Generation Partnership Project Long-Term Evolution) specify the use of pilot-assisted channel estimation (PACE) [1]. Pilot symbols or training sequences are known symbols either multiplexed with or superimposed onto the transmitted data in the time or frequency domain, with the associated disadvantage of a loss in spectral and/or power efficiency. Moreover, superimposed PACE is degraded at low signal-to-noise ratios, and multiplexed PACE is unsuitable for fast-fading channels with a coherence time shorter than the pilot-symbol transmission rate [2], [3].

*Blind channel-estimation methods* offer an alternative approach that avoids the implementation cost of pilot symbols [4]. Blind methods typically use second-order statistics of the received symbols for CSI estimation, with shortcomings such as increased complexity, slow convergence times, and channel-phase ambiguity [5]. In addition, the received *interference power spectral density* (PSD), which is due to both the thermal noise and the time-varying interference, is usually not estimated in the literature spanning both PACE and blind CSI estimation. The accuracy of the interference-PSD estimation is known to have a significant impact on turbo-principle (iterative) detection techniques as well as turbo and low-density parity-check (LDPC) channel decoding [6], [7].

The expectation-maximization (EM) algorithm offers a low-complexity iterative approach to optimal maximum-likelihood detection and estimation [8], [9]. A substantial body of literature can be found on EM-based techniques for data detection, multiuser detection, channel estimation, or a combination of the latter. A few representative examples are listed next. A recursive estimation of the fading channel amplitude was proposed in [10]. Iterative receivers with EM-based fading-amplitude and data estimation using pilot symbols for LDPC-based space-time coding and space-time block-coded orthogonal frequency-division multiplexing (OFDM) were studied in [11] and [12], respectively. Joint multiuser detection and channel/data estimation for uplink code-division multiple access (CDMA) was studied in [13]–[16]. In [17], iterative EM estimation and turbo coding were studied assuming noncoherent frequency-shift keying modulation and demodulation, which is well-known to be less power-efficient than coherent modulation [18].

Don Torrieri is with the US Army Research Laboratory, Adelphi, MD 20873 USA (email: dtorr@arl.army.mil).

Amitav Mukherjee is with the Department of Electrical Engineering and Computer Science, University of California, Irvine, CA 92617 USA (email: a.mukherjee@uci.edu).

Hyuck M. Kwon is with the Department of Electrical Engineering and Computer Science, Wichita State University, Wichita, KS 67260 USA (e-mail: hyuck.kwon@wichita.edu).

This work was partly sponsored by the Army Research Office under DEPSCoR ARO Grant W911NF-08-1-0256, and by NASA under EPSCoR CAN Grant NNX08AV84A.

In [19], an EM estimation approach for turbo-coded single-user iterative CDMA receivers with binary phase-shift keying was considered. In [20] and [21], the authors replaced turbo codes with regular LDPC codes; however, [19]–[21] all featured as much as a 9.1% pilot-symbol overhead for channel-amplitude and interference-PSD estimation. Recently, EM-based channel and noise estimation techniques were proposed in [22] and [23] for multiple-antenna systems with convolutional coding and as much as a 10% pilot-symbol overhead for initial channel estimation.

Although the primary role of pilot symbols in most cellular standards is channel estimation, pilot symbols often play a secondary role in cell, frame, or symbol synchronization. However, alternative methods of synchronization may be used when pilot symbols are unavailable [18], [24], [25]. In this paper, a doubly iterative direct-sequence CDMA (DS-CDMA) receiver featuring iterative EM channel estimation and iterative detection and decoding without *any* pilot symbols is presented. The general form of the proposed blind channel estimator provides fading-amplitude, phase, and interference-PSD estimates in both single-user and multiuser environments, therefore offering an alternative to the methods proposed in [26] and [27] to rectify the phase ambiguity of blind channel estimates<sup>1</sup>. The special case of EM channel estimation with perfect phase information at the receiver (e.g., by means of a phase-locked loop) is also considered. The proposed iterative receiver is capable of using higher-order modulations such as M-PSK and M-ary quadrature amplitude modulation (M-QAM), although quadriphase-shift keying (QPSK) is demonstrated in this work for simplicity. In addition, the proposed system uses irregular repeat-accumulate (IRA) codes instead of regular LDPC codes for lower complexity [28]–[30].

The paper is organized as follows. Section II describes the system transmitter and receiver models including coding, modulation, and spreading, as well as fading-channel parameters. Section III summarizes the proposed EM-based estimation process that uses soft feedback from the channel decoder. Section IV presents the proposed blind method for the initial CSI estimation and the possible trade-offs vis-à-vis PACE. Section V shows simulation results, and Section VI offers conclusions.

A word on notation: lowercase boldface is used to represent vectors, while uppercase boldface represent matrices.  $E$  denotes the statistical expectation,  $(\cdot)^T$  is the matrix transpose,  $*$  is the complex conjugate, and  $\lfloor x \rfloor$  is the largest integer smaller than  $x$ .

## II. SYSTEM MODEL

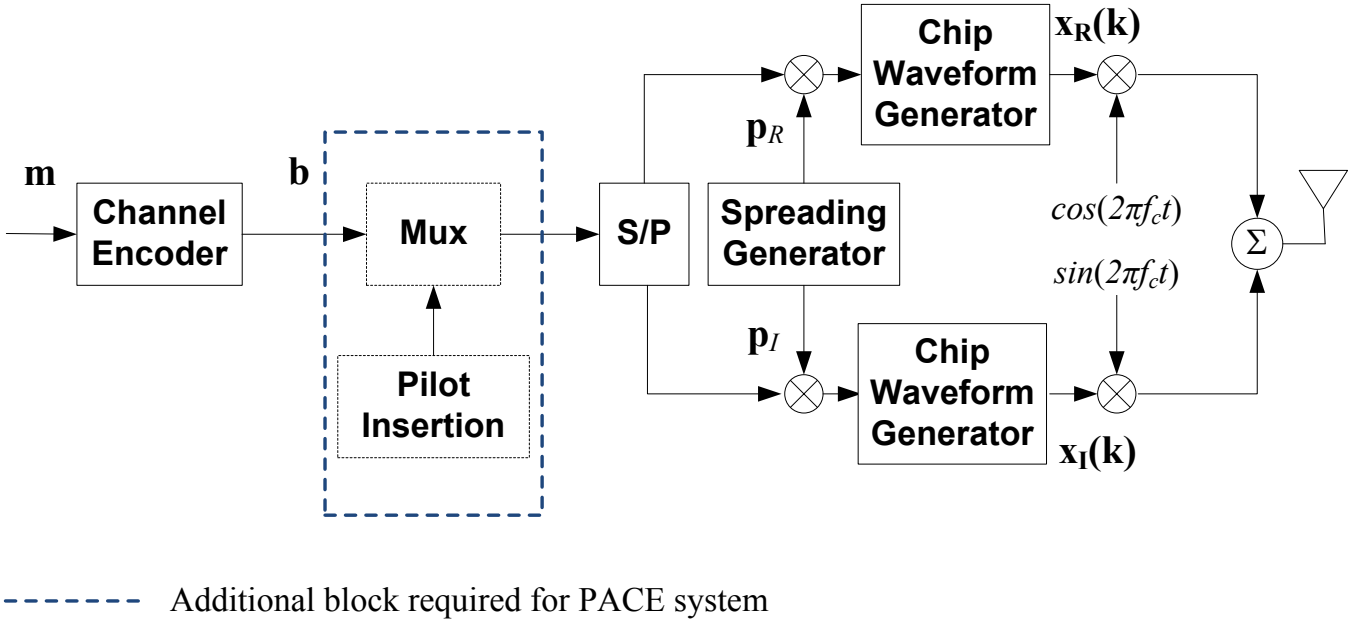


Fig. 1. DS-CDMA transmitter with QPSK modulation.

Fig. 1 shows the block diagram of a dual quaternary DS-CDMA transmitter [31] consisting of a channel encoder, QPSK modulator, and a direct-sequence spreading generator that multiplies orthogonal chip sequences  $\mathbf{p}_R$  and  $\mathbf{p}_I$  with the in-phase and quadrature modulator inputs. The input to the encoder in Fig. 1 is a binary, independent, identically distributed data block of length  $K$ , which is denoted by  $\mathbf{m} = [m(1), \dots, m(K)]$ ,  $m(i_{bit}) \in [1, 0]$ .

<sup>1</sup>In [26], two different PSK modulations are used on adjacent OFDM subcarriers to resolve the phase ambiguity under slow frequency-selective fading. A short pilot sequence is used in [27] to recover the channel phase, making it semi-blind in nature. More importantly, the interference-plus-noise PSD is not estimated in [26] and [27].

### A. Encoding, Modulation, and Spreading

Each  $1 \times K$  message vector  $\mathbf{m}$  is encoded into a  $1 \times N$  codeword  $\mathbf{b} = [b(1), \dots, b(N)]$  using a systematic, extended IRA code [28]. IRA codes offer a combination of the linear complexity of turbo encoding and the lower complexity of LDPC decoding without compromising on performance.

The  $(N, K)$  IRA code is constructed following the methodology proposed in [29], where the IRA code parameters were designed for use on a burst-erasure channel with additive noise, which was shown to be a good surrogate for Rayleigh fading channels. IRA codes can be considered to be a subset of low-density parity-check codes and therefore may be represented by a Tanner graph [30]. Let  $\lambda(x) = \sum_i^{d_v} \lambda_i x^{i-1}$  and  $\rho(x) = \sum_i^{d_c} \rho_i x^{i-1}$  represent the variable-node and check-node degree distributions of the code's Tanner graph, with  $(d_v, d_c)$  being the maximum variable and check node degrees, respectively. Using density evolution, for  $(d_v = 8, d_c = 7)$  we obtain the following good choices [29]:

$$\begin{aligned}\lambda(x) &= 0.00008 + 0.31522x + 0.34085x^2 + 0.006126x^6 \\ &\quad + 0.28258x^7 \\ \rho(x) &= 0.62302x^5 + 0.37698x^6.\end{aligned}\tag{1}$$

The  $(N - K) \times N$  IRA parity-check matrix can be represented as  $\mathbf{H} = [\mathbf{H}_1 \mid \mathbf{H}_2]$ , where sub-matrix  $\mathbf{H}_2$  is a  $(N - K) \times (N - K)$  dual-diagonal matrix, and  $\mathbf{H}_1$  is a randomly-generated  $(N - K) \times K$  sparse matrix constructed such that  $\mathbf{H}$  has the degree profile of (1). The  $K \times N$  systematic generator matrix  $\mathbf{G}$  is then given by  $\mathbf{G} = [\mathbf{I}_K \mid \mathbf{H}_1^T \mathbf{H}_2^{-T}]$ .

For the simulations in Section V, Gray-labeled QPSK is used with 2 encoded bits mapped into a modulation symbol  $x(k) \in \{\pm 1, \pm j\}$ ,  $k = 1, \dots, \frac{N}{2}$ . Although QPSK is assumed, the analysis and simulation is easily extended to M-QAM. Parallel streams of code bits are each spread using a Gold sequence with spreading factor  $g$  chips/code bit before rectangular pulse-shaping that produces the real and imaginary components of  $x(k)$ , i.e.,  $x_R(k) = \text{Re}(x(k))$  and  $x_I(k) = \text{Im}(x(k))$ . In practice, an intermediate frequency is used before the carrier frequency upconversion, but the upconversion from baseband to the intermediate frequency is omitted for clarity in Fig. 1.

No channel interleaving is applied to the IRA code due to the inherent interleaving characteristics of the IRA code itself. This is because the IRA code can be alternatively represented as a repetition code concatenated with a convolutional encoder (accumulator) with an interleaver between them. The interleaver is embedded within the sub-matrix  $\mathbf{H}_1$  in the Tanner graph representation of IRA codes.

### B. Channel Model

For multiple-access interference (MAI) environments, the channel coefficients are generated using the Jakes correlated fading model. The flat-fading assumption is valid when the information bit-rate is low, e.g., 100 kb/s as usually considered in this paper, since the multipath delay spread in a typical cellular environment is about 10  $\mu$ s, which is negligible compared to the symbol duration. For completeness, the proposed system and analysis are extended to include frequency-selective channels by including multipath components with delays exceeding a chip duration and using Rake receivers [18], [31], as described in Section V-E. Each codeword or frame of  $N$  code bits is divided into two different types of subframes or blocks. One block size is set equal to the  $n_{FB}$  code bits over which the fading amplitude is assumed to be constant. The other block size is set equal to  $n_{IB}$  code bits over which the interference level is assumed to be constant.

Each frame comprises  $N/2$  QPSK code symbols and  $Ng/2$  spreading-sequence chips for each QPSK component. The fading coefficient associated with spreading-sequence chip  $c$  of either  $\mathbf{p}_R$  or  $\mathbf{p}_I$  is

$$\begin{aligned}C_{\lfloor c/(n_{FB}g) \rfloor} &= \sqrt{E_s} \alpha_{\lfloor c/(n_{FB}g) \rfloor} e^{j\phi_{\lfloor c/(n_{FB}g) \rfloor}}, \\ c &= 1, \dots, \frac{Ng}{2}\end{aligned}\tag{2}$$

where  $E_s$  is the average energy per QPSK symbol,  $\alpha$  is the fading amplitude with  $E[\alpha^2] = 1$ , and  $\phi$  is the unknown fading-induced channel phase.

### C. Iterative Receiver Structure

Fig. 2 shows a block diagram of the proposed dual quaternary iterative receiver. The received signal is downconverted, passed through chip-matched filters, and despread by a synchronized spreading-sequence generator in each branch, with the downconverter and synchronization devices [18] omitted in Fig. 2 for clarity. Self-interference between the spreading sequences of the desired user is negligible because accurate synchronization is assumed at the receiver. Let  $N_0/2$  denote the two-sided PSD of the Gaussian noise. For the flat-fading scenario, the complex envelope of the desired user at the  $k^{th}$  symbol time with active MAI can be written as

$$y(k) = C_{\lfloor k/n_{FB} \rfloor} x(k) + n^{int}(k) + n(k), \quad 1 \leq k \leq \frac{N}{2}\tag{3}$$

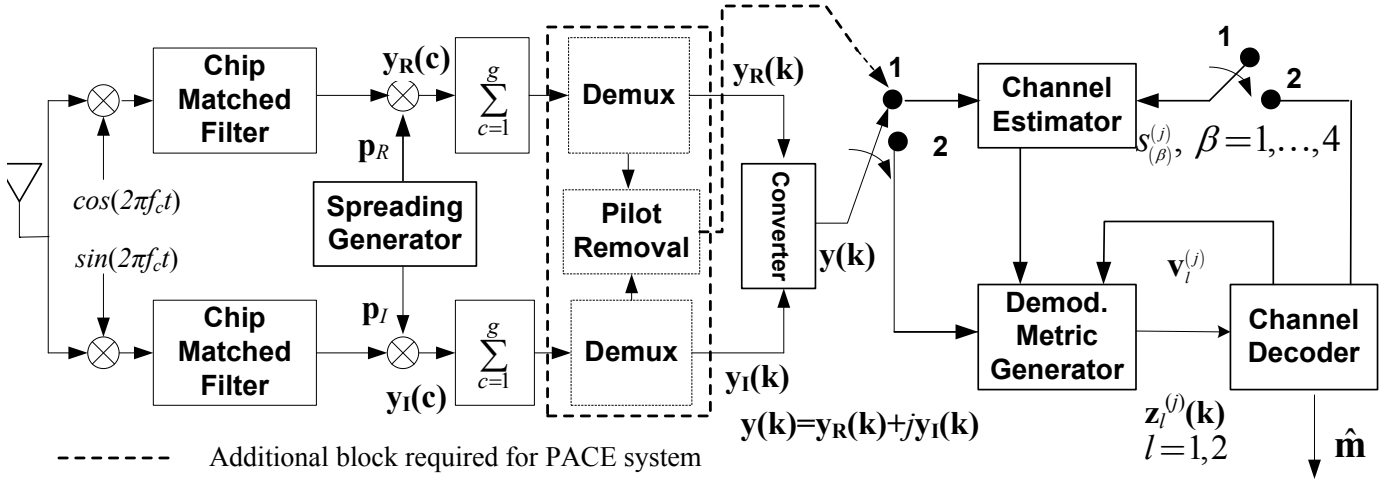


Fig. 2. Iterative DS-CDMA receiver.

where  $x(k)$  is the complex transmitted code symbol of the desired user,  $n(k)$  is a complex zero-mean circularly symmetric Gaussian noise sample with  $E[|n_k|^2] = N_0$ , and  $n^{int}(k)$  is the interference at the demodulator due to interfering users [18], [31].

The time-varying MAI is assumed to be generated by interfering users with a structure identical to the desired user, albeit the spreading sequences differ and the fading coefficients are independent. The despreading in the receiver tends to whiten the interference PSD over the code-symbol passband, and the subsequent filtering tends to produce a residual interference with a Gaussian distribution. Thus, the *interference PSD* due to the combined interference and thermal noise is modeled as additive Gaussian noise with a two-sided PSD  $I_0/2$  that is constant over each block of  $n_{IB}$  code bits but varies from block-to-block. This model enables the derivation of an EM estimator for  $I_0$  that is used in the demodulator metric and leads to the suppression of the interference.

A *receiver iteration* is defined as a fixed number of decoder iterations followed by internal EM iterations in the channel estimator of Fig. 2, and then a single demodulator metric generation. Let

$i$  denote the index for the internal EM iteration,  $i = 1, \dots, i_{max}$ ;

$j$  denote the index for the closed-loop receiver iteration,  $j = 1, \dots, j_{max}$ .

Let  $\hat{\theta}_{(i)}^{(j)} = (\hat{C}_{(i)}^{(j)}, \hat{I}_{0(i)}^{(j)})$  represent the estimates of the fading-coefficient and interference-PSD parameters at the  $i^{th}$  EM iteration during the  $j^{th}$  overall receiver iteration. EM iterations commence after the initial channel estimation and decoding, which is obtained while the switch in Fig. 2 is set to position 1. The subsequent receiver iterations are performed while the switch is set to position 2 in order to refine the initial channel estimate with the aid of soft feedback  $s_{\beta}^{(j)}$ ,  $\beta = 1, 2, 3, 4$  from the channel decoder.

### III. EM ALGORITHM

Theoretically, the maximum-likelihood CSI estimator  $\hat{\theta}$  can be obtained from a received data vector  $\mathbf{y} = [y(1), \dots, y(N_1)]$  of  $N_1$  code symbols, referred to as the *incomplete data*, by maximizing the conditional log-likelihood function:

$$\hat{\theta} = \arg \max_{\theta} \ln f(\mathbf{y} | \theta). \quad (4)$$

However, the computation of this equation is virtually prohibitive in practice since its complexity increases exponentially with the observation window size. In the EM algorithm, the expectation of the conditional log-likelihood of the *complete data*  $\mathbf{z} = (\mathbf{x}, \mathbf{y})$  is iteratively maximized with respect to  $\theta$ , where expectation is taken with respect to  $\mathbf{x}$  given  $\mathbf{y}$  and a previous estimate of  $\theta$ .

The conditional probability density function (pdf) of  $\mathbf{z}$  can be written as

$$f(\mathbf{z} | \theta) = f(\mathbf{x}, \mathbf{y} | \theta) = f(\mathbf{y} | \mathbf{x}, \theta) f(\mathbf{x} | \theta) = f(\mathbf{y} | \mathbf{x}, \theta) f(\mathbf{x}) \quad (5)$$

where the last equality is from the independence of the transmitted signal vector  $\mathbf{x}$  and the CSI parameter  $\theta$ . Thus,

$$\ln f(\mathbf{z} | \theta) = \ln f(\mathbf{y} | \mathbf{x}, \theta) + \ln f(\mathbf{x}). \quad (6)$$

Since the symbols are independent and circularly symmetric Gaussian noise and interference are assumed, the conditional pdf  $f(\mathbf{y} | \mathbf{x}, \boldsymbol{\theta})$  is

$$f(\mathbf{y} | \mathbf{x}, \boldsymbol{\theta}) = \frac{1}{(\pi I_0)^{N_1}} \exp \left( - \sum_{k=1}^{N_1} \frac{|y(k) - Cx(k)|^2}{I_0} \right). \quad (7)$$

Therefore, as  $|x(k)|^2 = 1 \quad \forall k$ ,

$$\begin{aligned} \ln f(\mathbf{y} | \mathbf{x}, \boldsymbol{\theta}) &= -N_1 \cdot \ln(I_0) - \frac{1}{I_0} \sum_{k=1}^{N_1} [|y(k)|^2 + |C|^2 \\ &\quad - 2 \operatorname{Re}(y^*(k)Cx(k))] \end{aligned} \quad (8)$$

where an irrelevant constant has been dropped.

**E-step:** Define the objective function to be the conditional expectation of the conditional log-likelihood of  $\mathbf{z} = (\mathbf{y}, \mathbf{x})$ , which can be written as

$$\chi(\boldsymbol{\theta}, \hat{\boldsymbol{\theta}}_{(i)}^{(j)}) = E_{\mathbf{z} | \mathbf{y}, \hat{\boldsymbol{\theta}}_{(i)}^{(j)}} [\ln f(\mathbf{z} | \boldsymbol{\theta})] \quad (9)$$

where  $\hat{\boldsymbol{\theta}}_{(i)}^{(j)}$  is the previous estimate. Using (6) and (8) and observing that  $\ln f(\mathbf{x})$  in (6) is independent of  $\boldsymbol{\theta}$ , and hence irrelevant to the maximization, we obtain

$$\begin{aligned} \chi(\boldsymbol{\theta}, \hat{\boldsymbol{\theta}}_{(i)}^{(j)}) &= -N/2 \cdot \ln(I_0) - \frac{1}{I_0} \sum_{k=1}^{N_1} [|y(k)|^2 + |C|^2 \\ &\quad - 2 \operatorname{Re}(y^*(k)C\bar{x}_{(i)}^{(j)}(k))] \end{aligned} \quad (10)$$

where  $\bar{x}_{(i)}^{(j)}(k) = E_{\mathbf{z} | \mathbf{y}, \hat{\boldsymbol{\theta}}_{(i)}^{(j)}} [x(k)] = E_{\mathbf{x} | \mathbf{y}, \hat{\boldsymbol{\theta}}_{(i)}^{(j)}} [x(k)]$ . Assuming the independence of each transmitted symbol  $x(k)$  and the independence of  $x(k)$  and  $\hat{\boldsymbol{\theta}}_{(i)}^{(j)}$ , and using Bayes' law and the fact that (7) can be expressed as a product of  $N_1$  factors, we obtain

$$\bar{x}_{(i)}^{(j)}(k) = E_{x(k) | y(k), \hat{\boldsymbol{\theta}}_{(i)}^{(j)}} [x(k)] \quad (11)$$

where

$$f(x(k) | y(k), \hat{\boldsymbol{\theta}}_{(i)}^{(j)}) = \frac{f(y(k) | x(k), \hat{\boldsymbol{\theta}}_{(i)}^{(j)})}{f(y(k) | \hat{\boldsymbol{\theta}}_{(i)}^{(j)})} \Pr(x(k)). \quad (12)$$

and

$$f(y(k) | x(k), \hat{\boldsymbol{\theta}}_{(i)}^{(j)}) = \frac{1}{\pi I_0} \exp \left( - \frac{|y(k) - Cx(k)|^2}{I_0} \right). \quad (13)$$

**M-step:** Taking the derivative of (10) with respect to the real and imaginary parts of the complex-valued  $C$ , and then setting the results equal to zero, we obtain the estimate of the fading coefficient at iteration  $i + 1$  as

$$\operatorname{Re}(\hat{C}_{(i+1)}^{(j)}) = \frac{1}{N_1} \sum_{k=1}^{N_1} \operatorname{Re}(y^*(k) \bar{x}_{(i)}^{(j)}(k)) \quad (14)$$

$$\operatorname{Im}(\hat{C}_{(i+1)}^{(j)}) = -\frac{1}{N_1} \sum_{k=1}^{N_1} \operatorname{Im}(y^*(k) \bar{x}_{(i)}^{(j)}(k)). \quad (15)$$

Similarly, maximizing (10) with respect to the interference PSD  $I_0$  leads to

$$\hat{I}_{0,(i+1)}^{(j)} = \frac{1}{N_1} \sum_{k=1}^{N_1} |y(k) - \hat{C}_{(i+1)}^{(j)} \bar{x}_{(i)}^{(j)}(k)|^2. \quad (16)$$

The fading phase and amplitude can be explicitly estimated from (14) and (15), but that is unnecessary.

Let  $s_{\beta}^{(j)}$ ,  $\beta = 1, 2, 3, 4$ , be the code-symbol probabilities obtained from the soft outputs of the channel decoder, with  $s_1 = \Pr(x(k) = +1)$ ,  $s_2 = \Pr(x(k) = +j)$ ,  $s_3 = \Pr(x(k) = -1)$ ,  $s_4 = \Pr(x(k) = -j)$ . From (7) and (12), the expectation of  $x(k)$  at the  $i^{th}$  EM and  $j^{th}$  receiver iteration is

$$\bar{x}_{(i)}^{(j)}(k) = \frac{s_1^{(j)} R_{1,(i)}^{(j)} + js_2^{(j)} R_{2,(i)}^{(j)} - s_3^{(j)} R_{3,(i)}^{(j)} - js_4^{(j)} R_{4,(i)}^{(j)}}{\sum_{\beta=1}^4 s_{\beta}^{(j)} R_{\beta,i}^{(j)}} \quad (17)$$

$$z_1^{(j)}(k) = \log \frac{\exp \left[ \frac{2}{\hat{I}_{0,(i_{\max})}^{(j)}} \operatorname{Im} \left( \hat{C}_{(i_{\max})}^{(j)} y^*(k) \right) \right] + \exp \left[ -\frac{2}{\hat{I}_{0,(i_{\max})}^{(j)}} \operatorname{Re} \left( \hat{C}_{(i_{\max})}^{(j)} y^*(k) \right) + v_2 \right]}{\exp \left[ \frac{2}{\hat{I}_{0,(i_{\max})}^{(j)}} \operatorname{Re} \left( \hat{C}_{(i_{\max})}^{(j)} y^*(k) \right) \right] + \exp \left[ -\frac{2}{\hat{I}_{0,(i_{\max})}^{(j)}} \operatorname{Im} \left( \hat{C}_{(i_{\max})}^{(j)} y^*(k) \right) + v_2 \right]} \quad (19)$$

$$z_2^{(j)}(k) = \log \frac{\exp \left[ -\frac{2}{\hat{I}_{0,(i_{\max})}^{(j)}} \operatorname{Im} \left( \hat{C}_{(i_{\max})}^{(j)} y^*(k) \right) \right] + \exp \left[ -\frac{2}{\hat{I}_{0,(i_{\max})}^{(j)}} \operatorname{Re} \left( \hat{C}_{(i_{\max})}^{(j)} y^*(k) \right) + v_1 \right]}{\exp \left[ \frac{2}{\hat{I}_{0,(i_{\max})}^{(j)}} \operatorname{Re} \left( \hat{C}_{(i_{\max})}^{(j)} y^*(k) \right) \right] + \exp \left[ \frac{2}{\hat{I}_{0,(i_{\max})}^{(j)}} \operatorname{Im} \left( \hat{C}_{(i_{\max})}^{(j)} y^*(k) \right) + v_1 \right]}. \quad (20)$$

where likelihood-ratio  $R_{\beta,(i)}^{(j)}$  depends on the current CSI estimates as

$$\begin{aligned} R_{1,(i)}^{(j)} &= \exp \left[ \frac{2}{\hat{I}_{0,(i)}^{(j)}} \operatorname{Re}(\hat{C}_{(i)}^{(j)} y(k)) \right] \\ R_{2,(i)}^{(j)} &= \exp \left[ \frac{2}{\hat{I}_{0,(i)}^{(j)}} \operatorname{Im}(\hat{C}_{(i)}^{(j)} y(k)) \right] \\ R_{3,(i)}^{(j)} &= \exp \left[ -\frac{2}{\hat{I}_{0,(i)}^{(j)}} \operatorname{Re}(\hat{C}_{(i)}^{(j)} y(k)) \right] \\ R_{4,(i)}^{(j)} &= \exp \left[ -\frac{2}{\hat{I}_{0,(i)}^{(j)}} \operatorname{Im}(\hat{C}_{(i)}^{(j)} y(k)) \right]. \end{aligned} \quad (18)$$

Therefore, for a given receiver iteration,  $\bar{x}_{(i)}^{(j)}(k)$  and  $R_{\beta,i}^{(j)}$  are updated  $i_{\max}$  number of times using decoder feedback  $s_{\beta}^{(j)}$ . In the next receiver iteration, after channel re-estimation, the fading-coefficient and interference-PSD estimates are updated, and then used at the demodulator and channel decoder to recompute  $\bar{x}_{(i)}^{(j+1)}(k)$  and  $R_{\beta,i}^{(j+1)}$ . This process is repeated again for  $i_{\max}$  EM iterations, and the aforementioned cycles continue likewise for subsequent receiver iterations.

In estimating the fading parameters, we set  $N_1 = n_{FB}/2$ ; in estimating  $I_0$ , we choose  $n_{IB} \leq n_{FB}$  and set  $N_1 = n_{IB}/2$ . The EM estimator first finds the value of  $\hat{C}_{(i)}^{(j)}$  for a fading block of size  $n_{FB}$ . Then it finds the value of  $\hat{I}_{0,(i)}^{(j)}$  for each smaller or equal interference block of size  $n_{IB}$  using the value of  $\hat{C}_{(i)}^{(j)}$  found for the larger or equal fading block. When pilot symbols are used, we set  $\bar{x}_{(i)}^{(j)}(k) = x(k)$  for each known pilot bit, and there are no EM iterations if only known pilot bits are processed in calculating the channel estimates. The application of the EM algorithm is to obtain both channel-coefficient and interference-PSD estimates, which differs from [11]–[13] where the emphasis is on data detection, and noise statistics are assumed to be perfectly known.

Let  $l = 1, 2$  denote the two bits of a QPSK symbol, and  $v_1, v_2$  denote the corresponding log-likelihood ratios that are fed back by the channel decoder. From [21] and [32, Eqn. 6], the demodulation metrics (extrinsic information)  $z_l^{(j)}(k), l = 1, 2$  for bits 1, 2 of symbol  $k$  that are applied to the channel decoder are shown at the top of the next page.

The number of EM iterations and the receiver latency are reduced by applying a *stopping criterion*. Iterations stop once  $\hat{C}_{(i)}^{(j)}$  is within a specified fraction of its value at the end of the previous iteration or a specified maximum number is reached. The fraction should be sufficiently small (perhaps 10%) that the performance loss will be insignificant.

#### IV. BLIND CSI ESTIMATION

The EM algorithm in Section III generates updated CSI estimates as shown in (14)–(16) *after* the initial coherent demodulation and decoding of receiver iteration  $j = 0$ . In [19]–[21], the initial CSI estimates were obtained with the aid of pilot symbols. In this section, two methods for blind estimation of the initial CSI parameters  $\hat{\theta}_{(i_{\max})}^{(0)} = \left( \hat{C}_{(i_{\max})}^{(0)}, \hat{I}_{0(i_{\max})}^{(0)} \right)$  are presented, with the special case of perfect phase information at the receiver examined first.

##### A. Perfect Phase Information at Receiver

The carrier synchronization provided by a phase-locked loop in several second and third-generation cellular standards such as IS-95 and CDMA20001x can be exploited to obviate the need to estimate the channel phase (which is also potentially provided by 2% piloting [27]). Assuming perfect phase information at the receiver, the fading amplitude is real-valued and nonnegative,

and (15) does not have to be computed. A simple heuristic estimate (denoted as *blind method I*) of  $(\hat{C}_{(i_{max})}^{(0)}, \hat{I}_{0,(i_{max})}^{(0)})$  for each fading block can be obtained from the received symbols as

$$\hat{C}_{(i_{max})}^{(0)} = \frac{2}{n_{FB}} \sum_{k=1}^{n_{FB}/2} |y(k)| \quad (21)$$

$$\hat{I}_{0,(i_{max})}^{(0)} = \max \left[ D - \left( \hat{C}_{(i_{max})}^{(0)} \right)^2, h \cdot \left( \hat{C}_{(i_{max})}^{(0)} \right)^2 \right] \quad (22)$$

where

$$D = \frac{2}{n_{FB}} \sum_{k=1}^{n_{FB}/2} |y(k)|^2 \quad (23)$$

represents the average power of the received symbols, and  $D - \left( \hat{C}_{(i_{max})}^{(0)} \right)^2$  is the difference between that power and the estimated average power of a desired symbol. Equation (21) would provide a perfect estimate in the absence of noise and interference. The parameter  $h > 0$  is chosen such that  $\left( \hat{C}_{(i_{max})}^{(0)} \right)^2 / \hat{I}_{0,(i_{max})}^{(0)}$  does not exceed some maximum value. Ideally,  $h$  is a function of  $E_s/N_0$ , but in this paper a constant  $h = 0.1$  is always used for simplicity.

### B. Complexity Analysis

Although the EM estimation is a relatively low-complexity iterative approach to maximum-likelihood estimation, it consumes a much larger number of floating-point operations than pilot-assisted schemes do. To evaluate the complexity of the EM estimator in terms of required real additions and multiplications per block of  $N_1$  code symbols, each complex addition is equated to two real additions, each complex multiplication is equated to four real multiplications, and divisions are equated with multiplications. Equations (14)–(16) require  $j_{\max} i_{\max} (6N_1 + 4)$  real additions and  $j_{\max} i_{\max} (12N_1 + 4)$  real multiplications. Equations (18) and (19) require  $6j_{\max} i_{\max}$  real additions,  $30j_{\max} i_{\max}$  real multiplications, and the computation of 4 exponentials. The initial estimates calculated using (21)–(23), which only need to be computed once prior to the first EM iterations, require  $2N_1$  real additions,  $8N_1 + 7$  real multiplications, and the computation of the maximum of two real numbers. A PACE receiver that uses only pilot symbols for CSI estimation requires  $6N_1 + 4$  real multiplications and  $12N_1 + 4$  real multiplications to compute (14)–(16) once and does not need to compute the other equations. Thus, EM estimation increases the amount of computation for CSI estimation by a factor of more than  $j_{\max} i_{\max}$  relative to PACE.

### C. No Phase Information at Receiver

The initial CSI estimates proposed in (21) and (22) for blind method I are expected to be degraded significantly when the phase information is also unknown, since an arbitrary initial phase value (e.g., 0 radians) must be assumed. To circumvent this problem, the initial receiver iteration consists of hard-decision demodulation and channel decoding, after which each decoded bit is used as  $\bar{x}_{(i_{max})}^{(0)}(k)$  in (14)–(16). This step is followed by the regular EM estimation process in subsequent receiver iterations. This approach for the initial CSI estimates, which is referred to as *blind method II* in the sequel, results in increased receiver latency relative to the previous method when phase information is not available.

### D. Blind-PACE Estimation Tradeoffs

The previously proposed iterative DS-CDMA receiver with PACE [19]–[21] is considered as the benchmark for comparison with the proposed receiver. Assuming an identical transmit-power constraint and information bit-rate in both cases, the elimination of pilots creates the following possibilities for methods I and II:

- (Case A) An increase in the number of transmitted information symbols.
- (Case B) An increase in transmitted information-symbol duration.
- (Case C) An increase in the number of transmitted parity symbols (lowered IRA code rate).

The modifications listed above offset the loss in system performance due to the degraded CSI estimation obtained from blind methods I and II with respect to PACE. The no-pilot cases A, B, and C have the same transmitted frame duration as the frame with pilot symbols. Cases A, B, and C provide the most favorable throughput, spectral efficiency, and bit error rate, respectively. Numerical evaluations of each of these cases are presented in the next section. Although a correlated fading model is assumed in the simulations, no filtering is used to exploit this correlation in order to maintain the robustness of the proposed estimator.

## V. SIMULATION RESULTS

In all the simulations, the block sizes are equal, and the information-bit rate is 100 kb/s. Increasing the block sizes increases the accuracy of the EM estimators, but decreasing the block sizes allows closer tracking of the channel parameters and includes more diversity in the receiver computations. In most of the simulations, except where stated, we set  $n_{FI}=n_{FB}=40$  and spreading factor  $g=31$ . The number of closed-loop receiver iterations is set to  $j_{max}=9$ , as there is insignificant performance improvement for  $j_{max}>9$ . The number of internal EM iterations is  $i_{max}=10$ . There is one decoder iteration per receiver iteration. A IRA code (data block size  $K=1000$ ) with sum-product algorithm decoding [18] is used without channel interleaving. The IRA code is rate-1/2 when PACE is used. Jakes correlated fading of the desired signal and a mobile velocity of 120 km/hr are assumed. Flat fading is assumed in most of the simulations, whereas a frequency-selective channel is examined in Section V-E. The iterative PACE receiver considered for comparison contains 9.1% pilot-symbol overhead, which has been shown to have a decoding performance close to the conventional 3GPP LTE receiver [21]. For each scenario tested, 5000 Monte Carlo simulation trials were conducted. To avoid repetition, a selection of representative examples out of the many possible combinations of channel coding, phase information, interference models, and no-pilot modifications are presented next.

The bit error rate (BER) is calculated as a function of  $E_b/N_0$ , where  $E_b=(N/2K)E_s$  is the energy per bit. The information throughput is a vital performance criterion in addition to the BER. One of the primary motivations in removing pilot symbols is the expectation of achieving greater throughput, even though the BER performance may be degraded marginally. We define throughput  $R$  as

$$R = \frac{\text{information bits in a codeword}}{\text{codeword duration}} \times (1 - BER) \quad \text{bits/s.} \quad (24)$$

### A. Single-user environment, perfect phase knowledge

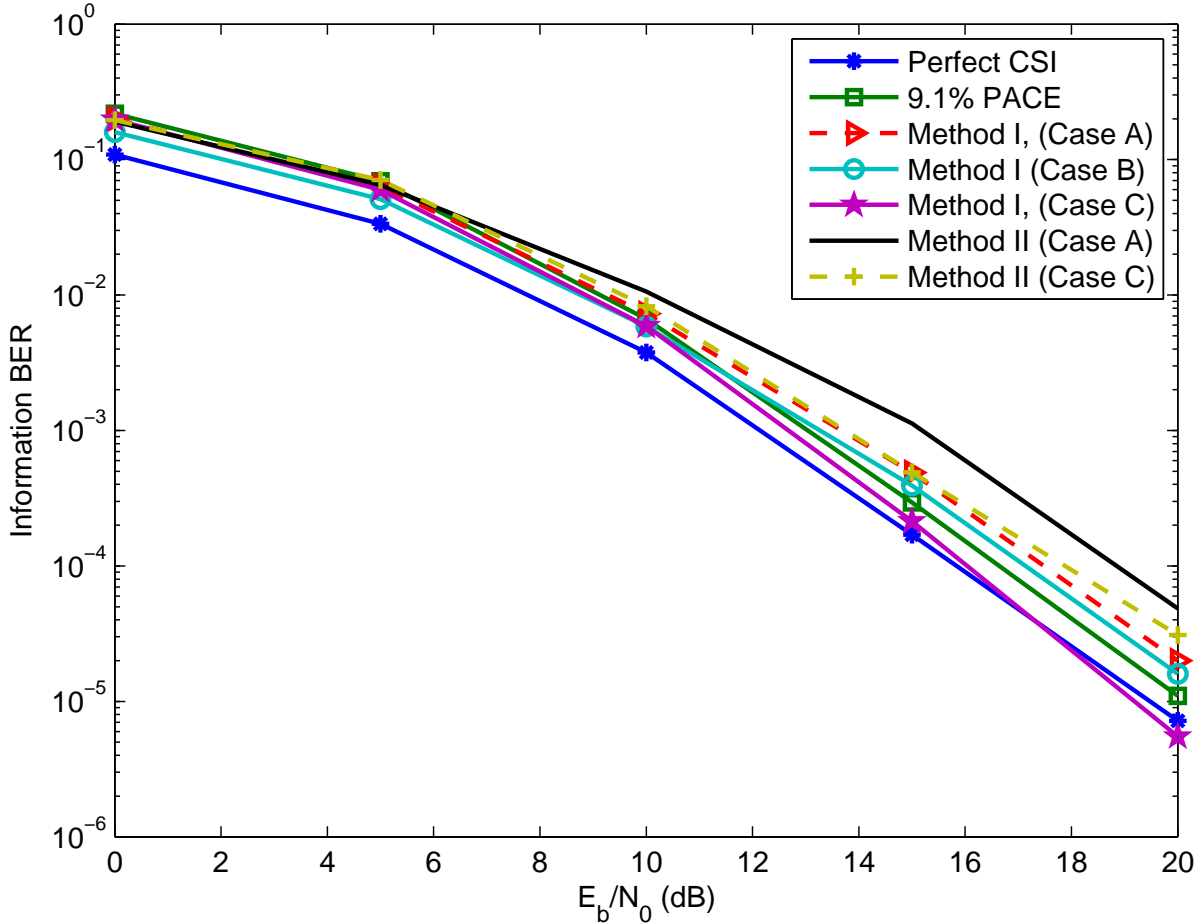


Fig. 3. BER versus  $E_b/N_0$  for IRA-coded iterative receiver in single-user environment with phase provided by PLL.



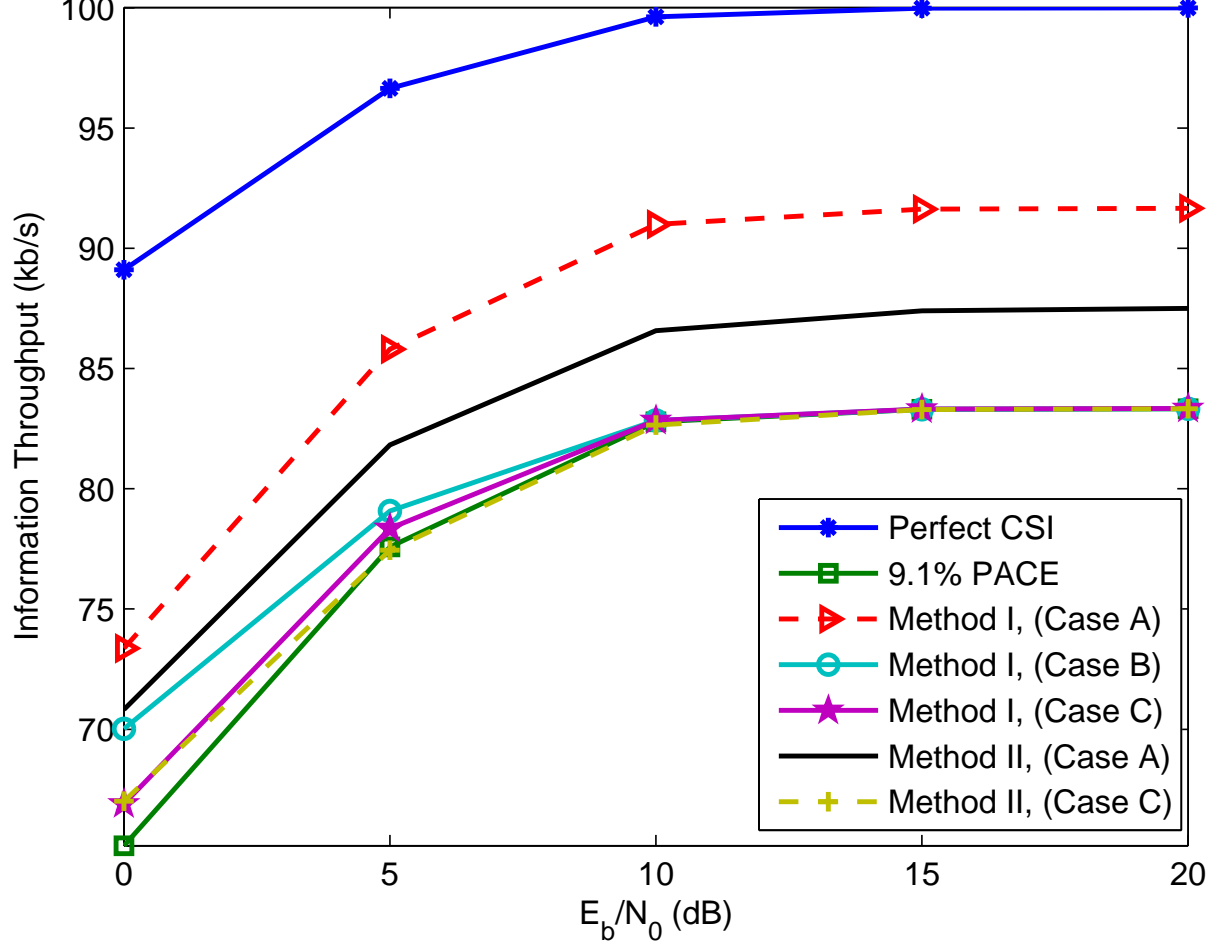


Fig. 4. Information throughput versus  $E_b/N_0$  for IRA-coded iterative receiver in single-user environment with phase provided by PLL.

For the first set of results in Figs. 3–4, a single-user environment and perfect phase knowledge at the receiver are assumed. Fig. 3 displays the BER versus  $E_b/N_0$  for an IRA-coded iterative receiver operating with perfect CSI, PACE, blind method I with cases A, B, and C, and blind method II with cases A and C, respectively. The key observation is that blind method II is worse than method I by 2 dB at  $BER = 10^{-3}$  for both case A and case C, which illustrates the well-known sensitivity of the EM algorithm to the accuracy of the initial estimates.

The addition of extra parity bits to blind method I (case C, rate-1000/2200) offers the greatest improvement in BER, surpassing even the rate-1/2 code with perfect CSI at high  $E_b/N_0$ . The increase in number of information symbols (case A) results in the worst BER performance with a separation of 1 dB and 0.5 dB from PACE and case B at  $BER = 10^{-3}$ , respectively.

The various scenarios featured in Fig. 3 were also tested under a slow-fading channel with mobile velocity of 10 km/hr. It was observed that all the BER curves were shifted towards the right by up to 7 dB at  $BER = 10^{-3}$ , but the overall trends among the different cases remained the same.

Fig. 4 exhibits information throughput  $R$  versus  $E_b/N_0$  for the IRA-coded iterative receiver with the scenarios of Fig. 3. The throughput advantage of case A is achieved even though no pilot symbols are used at all; i.e., the initial estimation is totally blind. It is evident that increasing the symbol duration or adding additional parity information does not give the proposed blind methods any significant advantage in throughput over PACE. Both blind methods with cases B, C and PACE provide about 20% less throughput than the receiver with perfect CSI.

#### B. Multiuser environment, unknown phase

A 4-user interference environment with equal mean bit energies for all users at the receiver,  $E_b/N_0 = 20$  dB, and no phase information at the receiver is examined next. It is assumed that both the interference levels and the unknown phase are constant during each subframe. Each interference signal experiences independent Jakes correlated fading and uses independent

data and Gold sequences with respect to the desired signal. The simulation uses chip-synchronous interference signals, which is a pessimistic worst-case assumption [31]. Two variations of CSI estimation are examined here: *partially adaptive* with only fading coefficient  $\hat{C}_{(i)}^{(j)}$  being estimated using (14), (15), and  $\hat{I}_{0(i)}^{(j)}$  set equal to  $N_0$  for all subframes; and *fully adaptive* estimation of both  $\hat{C}_{(i)}^{(j)}$  and  $\hat{I}_{0(i)}^{(j)}$  using (14), (15), and (16).

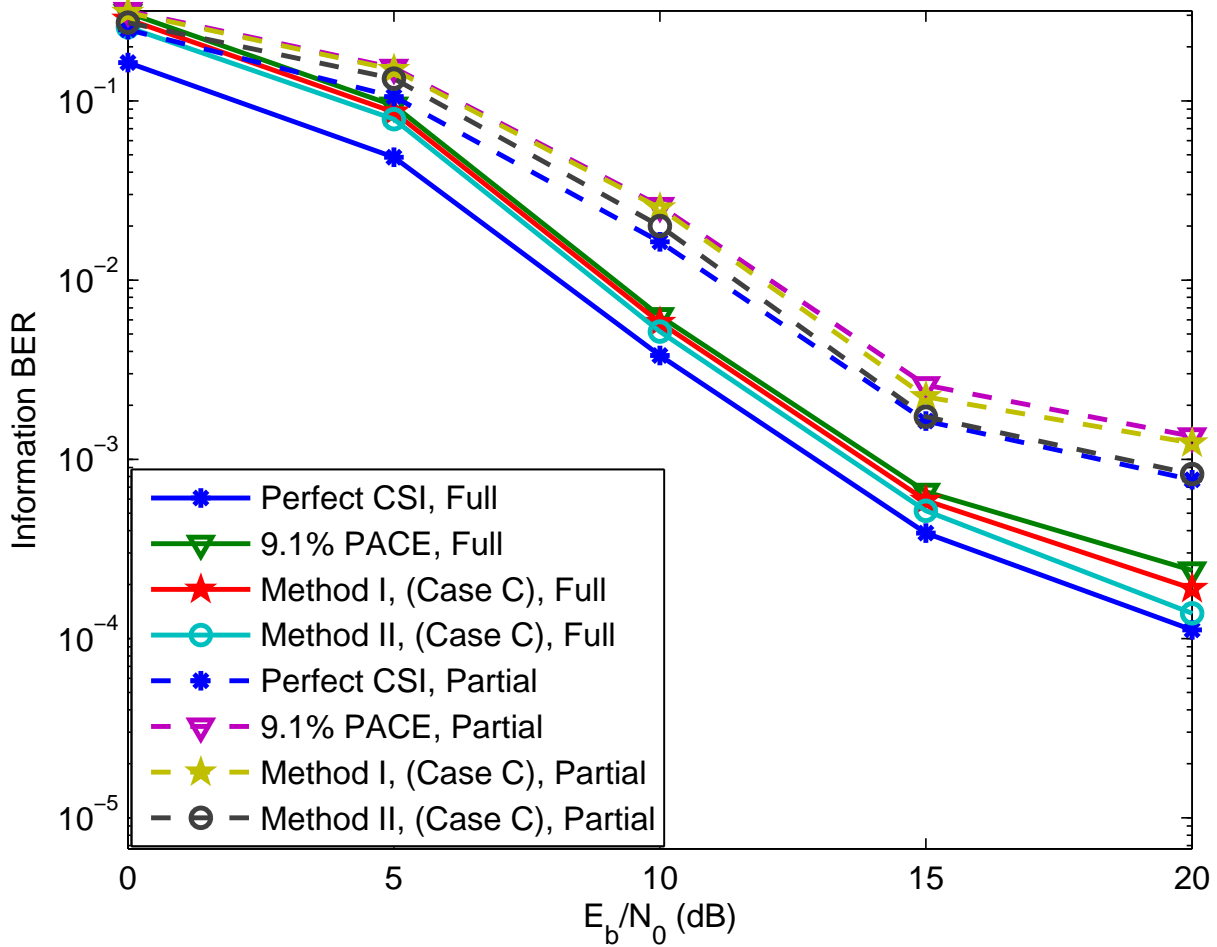


Fig. 5. BER versus  $E_b/N_0$  for IRA-coded iterative receiver affected by MAI from 4 users, fully and partially adaptive estimation, and unknown phase.

Fig. 5 displays IRA-coded BER versus  $E_b/N_0$  for partially and fully adaptive CSI estimation per fading block and case C for both blind methods. The mismatch of  $\hat{I}_0$  and the true value of  $I_0$  at the demodulator and decoder results in a high error floor for the partially adaptive cases. The intuition behind the error floor is that the partially adaptive estimator overestimates the true signal-to-interference-plus-noise ratio (SINR) by disregarding the MAI, with the degree of overestimation increasing with SINR. For IRA codes, it was shown in [33] that both under- and overestimation of the SINR degrades the IRA decoder performance. The fully adaptive estimation offers a more accurate SINR estimate and, hence, suppresses interference and reduces the error floor significantly. This interference suppression is achieved without using the far more elaborate multiuser and signal cancellation methods that could be implemented in a DS-CDMA receiver. For both partially and fully adaptive estimation, it is observed that blind method II now outperforms method I due to better phase estimation, whereas both blind methods outperform PACE at  $BER = 10^{-3}$  due to the added parity information.

Fig. 6 demonstrates the IRA-coded receiver throughput offered by the proposed methods under MAI from 4 users. The blind methods always provide a better throughput compared with PACE; for example, method I with case A is superior by 9% to both PACE scenarios when  $E_b/N_0 > 5$  dB. It is observed that both partial and fully-adaptive estimation methods offer a similar asymptotic throughput, which indicates that partial CSI estimation may be sufficient for applications with a non-stringent BER criterion. On the other hand, error-critical applications requiring less than  $BER = 10^{-3}$  must use the fully adaptive CSI estimation, as seen from Fig. 5.

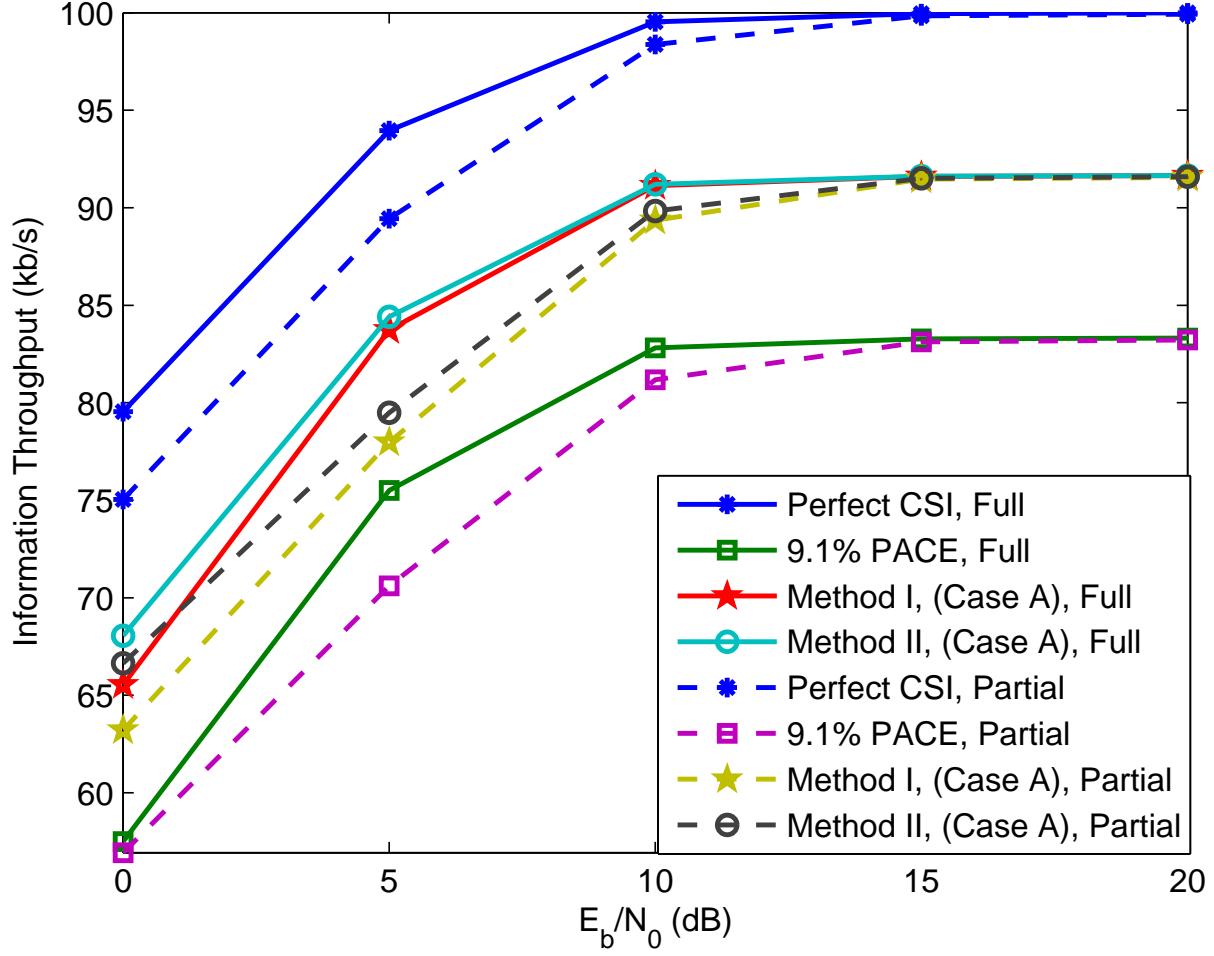


Fig. 6. Information throughput versus  $E_b/N_0$  for IRA-coded iterative receiver affected by MAI from 4 users, fully and partially adaptive estimation, and unknown phase.

### C. Varying fading-block size, unknown phase

In urban mobile environments, the phase can be expected to change significantly after approximately  $\frac{0.01}{f_d}$  s to  $\frac{0.04}{f_d}$  s, where  $f_d$  is the maximum Doppler shift. For the assumed mobile velocity of 120 km/hr, this time range corresponds to roughly 10 to 40 code bits at 100 kb/s. The fading and interference block sizes  $n_{FB} = n_{IB}$  are therefore varied accordingly, and *no* phase information is assumed to be available at the receiver for the next set of results.

Fig. 7 displays fully adaptive IRA-coded BER versus  $E_b/N_0$  for blind methods I and II with case *C*, 9.1 % PACE, and perfect CSI decoding for  $n_{FB} = 10$  and 40 in a single-user environment. An improvement of 1 to 2 dB was observed for all methods for the smaller fading-block size of  $n_{FB} = 10$  due to the increased fading diversity. The throughput with case *A* is shown in Fig. 8. It is observed that the throughput gains of the proposed blind methods over PACE (roughly 9% at intermediate to high  $E_b/N_0$ ) are preserved even when the phase is initially unknown at the receiver.

### D. Varying MAI, unknown phase

IRA-coded iterative receiver performance with blind method II, case *C* is examined for 3 and 6 MAI signals with equal mean bit energies for all users at the receiver in Fig. 9. The partially adaptive estimation is unable to cope with the interference caused by 6 MAI signals regardless of the spreading factor, whereas the fully adaptive estimation offers a substantial improvement in BER. The benefit of an increased spreading factor ( $g = 127$  versus  $g = 31$ ) is more apparent at low bit error rates for fully adaptive estimation. For example, the fully adaptive estimation with 3 MAI signals improves by a factor of approximately 5 dB at  $BER = 10^{-5}$ , despite nonorthogonal spreading sequences and imperfect CSI.

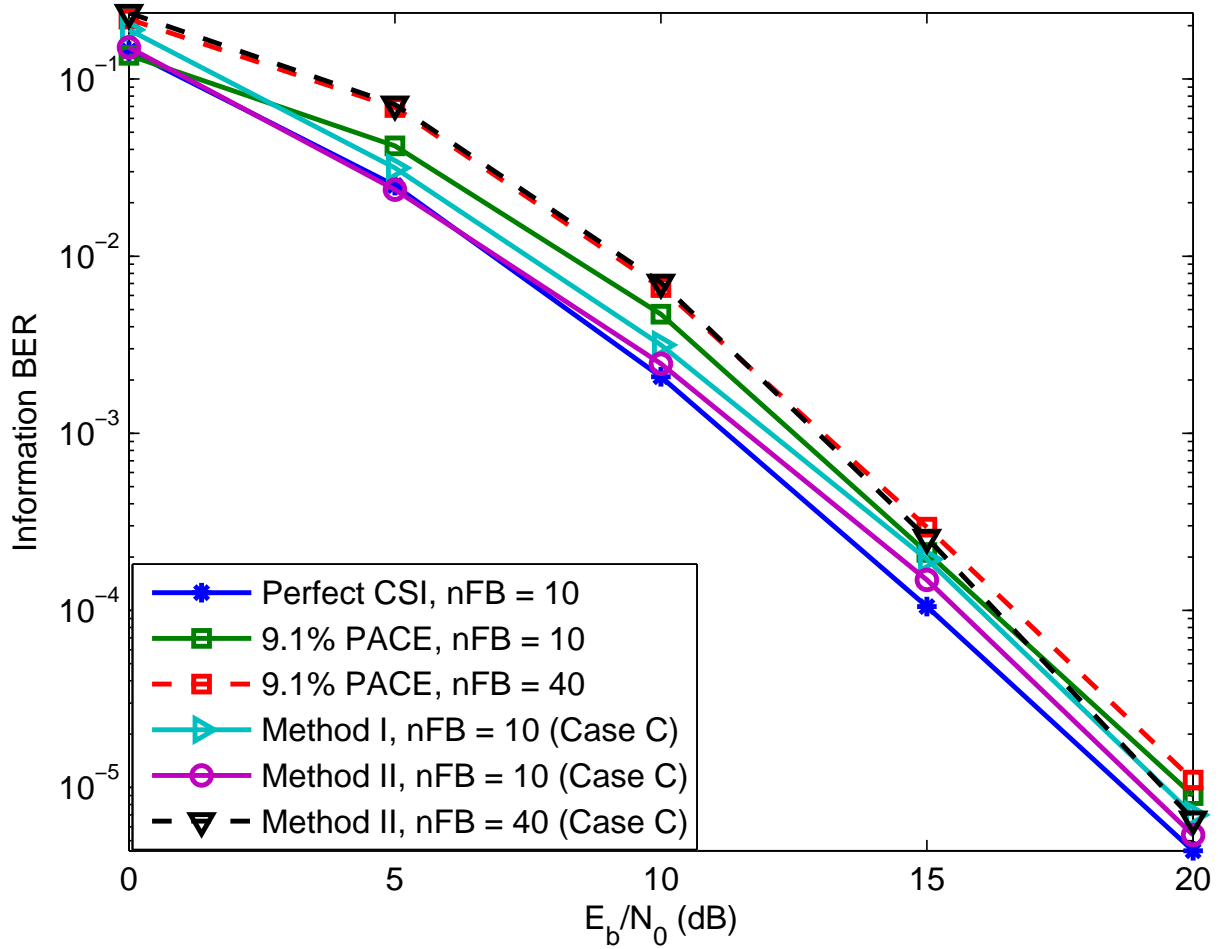


Fig. 7. BER versus  $E_b/N_0$  for IRA-coded iterative receiver in single-user environment, varying  $n_{FB}$ , and unknown phase.

#### E. Multipath channel

A DS-CDMA system can exploit a frequency-selective fading channel by using a Rake receiver. As an example, we assume a channel with three resolvable multipath components (with known delays) of the desired signal and a Rake combiner with three corresponding fingers. The multipath components undergo independent fading across the fingers, but follow the Jakes correlated fading assumption over time. The multipath components follow an exponentially decaying power profile across the fingers, i.e.,  $E[\alpha_l]^2 = e^{-(l-1)}$ ,  $l = 1, 2, 3$ . Each interference signal has the same power level in each finger and undergoes independent Jakes correlated fading. The assumption of independent multipath fading amplitude and phase coefficients for the desired signal allows us to apply the proposed EM-based channel estimation scheme separately in each finger. The Rake combiner performs maximal-ratio combining (MRC) of the received symbol copies based on channel and interference-PSD estimates computed at all fingers. The MRC decision statistic obtained from the Rake combiner is then passed to the QPSK demodulator metric generator, which generates soft inputs for the common channel decoder. The channel decoder soft outputs are fed back to the three channel estimator blocks, which then recompute updated channel coefficients, as described in Section III.

Fig. 10 displays the Rake receiver performance for various levels of MAI with Method II under case C, where all users have length-127 Gold sequences. It is observed that the additional diversity due to Rake combining improves performance as expected, but the performance disparity between partially and fully adaptive estimation remains large.

## VI. CONCLUSIONS

It has been shown that pilot symbols are not essential to the effectiveness of DS-CDMA receivers with coding, coherent detection, and channel estimation. If the pilot symbols are replaced by information symbols, the throughput increases relative to PACE whether or not interference is present. If the BER is the primary performance criterion, then replacing the pilot symbols by parity symbols gives a lower BER than PACE. If the spectral efficiency is of primary importance, then extending

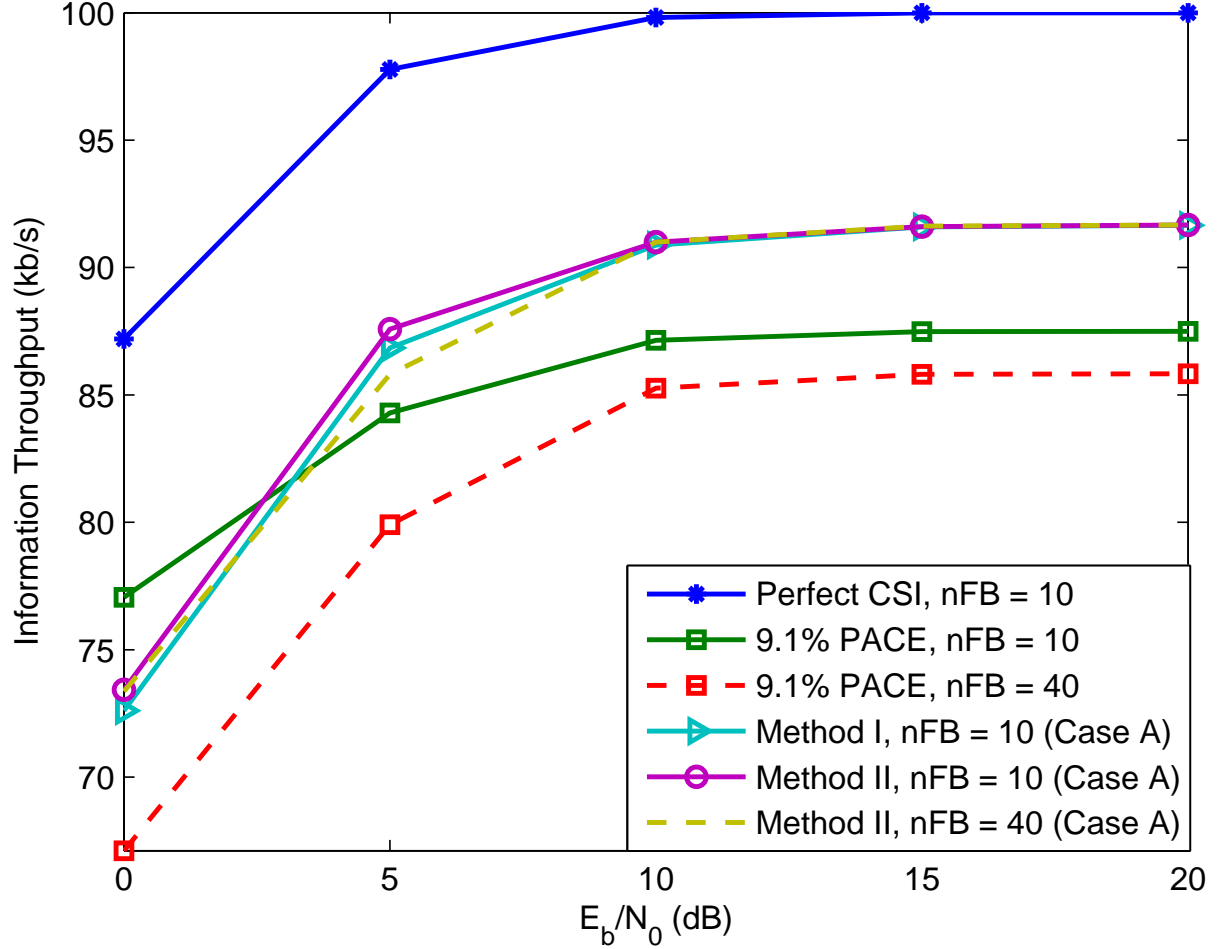


Fig. 8. Information throughput versus  $E_b/N_0$  for IRA-coded iterative receiver in single-user environment, varying  $n_{FB}$ , and unknown phase.

the symbol duration after the removal of the pilot symbols offers an improvement relative to PACE, albeit at the cost of a slight increase in the BER.

The estimation of the interference PSD has been shown to enable the significant suppression of interference. This suppression is achieved without using the far more elaborate multiuser and signal cancellation methods that could be implemented in a DS-CDMA receiver.

#### ACKNOWLEDGMENT

The second author would like to thank Avinash Mathur for his assistance in the early stages of this work.

#### REFERENCES

- [1] 3GPP *Physical Channels and Modulation* [Online]. Available: <http://www.3gpp.org/ftp/Specs/archive/36%5Fseries/36.211/>
- [2] J. K. Cavers, "An analysis of pilot symbol assisted modulation for Rayleigh fading channels," *IEEE Trans. Veh. Tech.*, vol. 40, pp. 686 - 693, Nov. 1991.
- [3] P. Hoeher and F. Tufvesson, "Channel estimation with superimposed pilot sequence," in *Proc. IEEE GLOBECOM*, pp. 2162 - 2166, 1999.
- [4] L. Tong, G. Xu, and T. Kailath, "Blind identification and equalization based on second-order statistics: A time domain approach," *IEEE Trans. Inf. Theory*, vol. 40, pp. 340 - 349, Mar. 1994.
- [5] X. Wang and H. V. Poor, "Blind adaptive multiuser detection in multipath CDMA channels based on subspace tracking," *IEEE Trans. Signal Process.*, vol. 46, pp. 3030 - 3044, Nov. 1998.
- [6] T. A. Summers and S. G. Wilson, "SNR mismatch and online estimation in turbo decoding," *IEEE Trans. Commun.*, vol. 46, pp. 421 - 423, Apr. 1998.
- [7] D. J. MacKay and C. P. Hesketh, "Performance of low density parity check codes as a function of actual and assumed noise levels," *Electr. Notes Theor. Comput. Sci.*, vol. 74, pp. 89 - 96, 2003.
- [8] G. J. McLachlan and T. Krishnan, *The EM Algorithm and Extensions*, Wiley, 1997.
- [9] A. P. Dempster, N. M. Laird, and D. B. Rubin, "Maximum-likelihood from incomplete data via the EM algorithm," *J. Roy. Stat. Soc.*, vol. 39, pp. 1 - 38, 1977.
- [10] H. Jafarian and S. Pasupathy, "EM-based recursive estimation of channel parameters," *IEEE Trans. Commun.*, vol. 47, pp. 1297 - 1302, Sep. 1999.

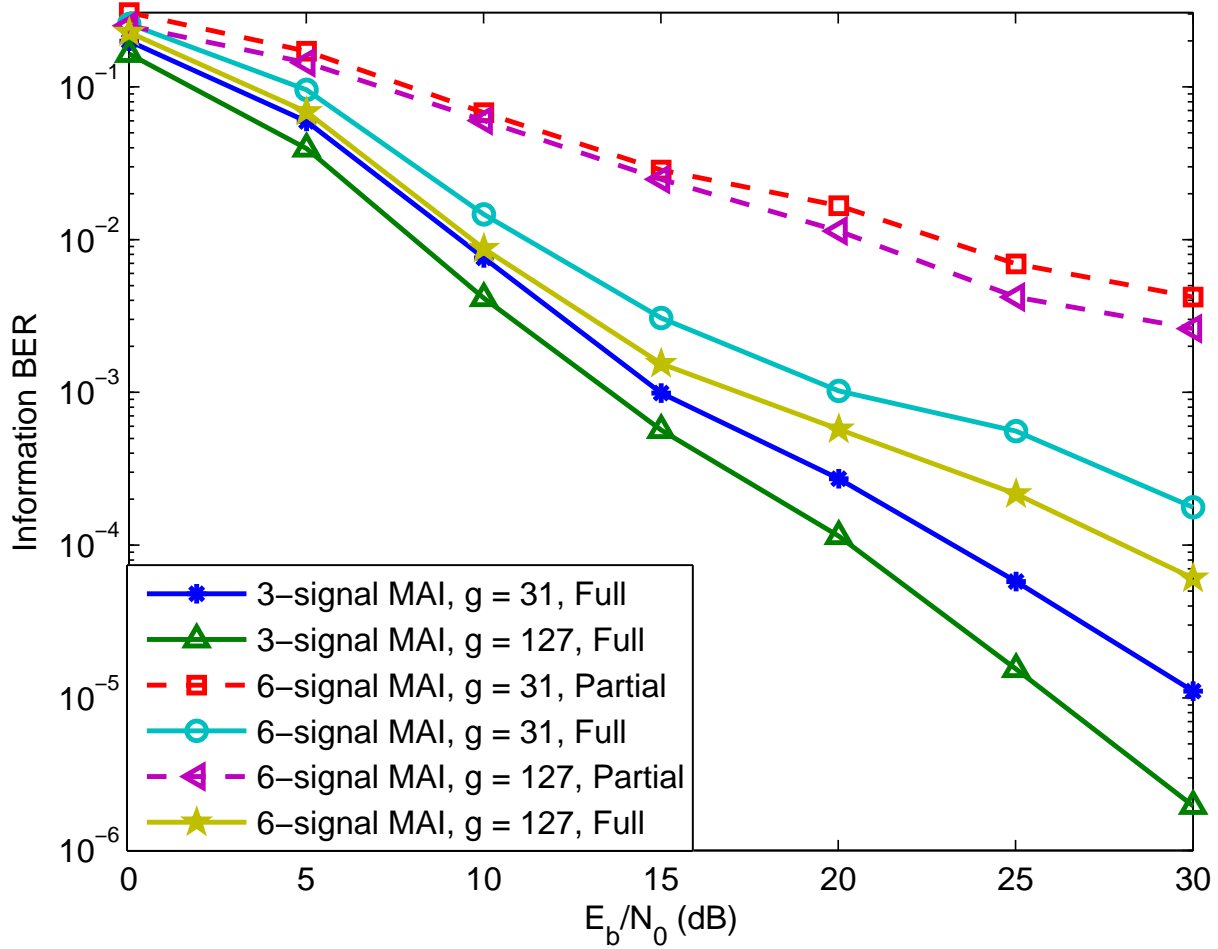


Fig. 9. BER versus  $E_b/N_0$  for IRA-coded iterative receiver affected by an unknown phase and various spreading factors, MAI levels, and degrees of adaptation.

- [11] B. Lu, X. Wang, and K. R. Narayanan, "LDPC-based space-time coded OFDM systems over correlated fading channels: Performance analysis and receiver design," *IEEE Trans. Commun.*, vol. 50, pp. 74 - 88, Jan. 2002.
- [12] B. Lu, X. Wang, and Y. Li, "Iterative receivers for space-time block coded OFDM systems in dispersive fading channels," *IEEE Trans. Wireless Commun.*, vol. 1, pp. 213 - 225, Apr. 2002.
- [13] A. Kocian and B. H. Fleury, "EM-based joint data detection and channel estimation of DS-CDMA signals," *IEEE Trans. Commun.*, vol. 51, pp. 1709 - 1720, Oct. 2003.
- [14] L. B. Nelson and H. V. Poor, "Iterative multiuser receivers for CDMA channels: An EM-based approach," *IEEE Trans. Commun.*, vol. 44, pp. 1700 - 1710, Dec. 1996.
- [15] M. Kobayashi, J. Boutros, and G. Caire, "Successive interference cancellation with SISO decoding and EM channel estimation," *IEEE J. Sel. Areas Commun.*, vol. 19, pp. 1450 - 1460, Aug. 2001.
- [16] S. Wu, U. Mitra, and C.-C. Jay Kuo, "Iterative joint channel estimation and multiuser detection for DS-CDMA in frequency-selective fading channels," *IEEE Trans. Signal Process.*, vol. 56, pp. 3261 - 3277, Jul. 2008.
- [17] S. Cheng, M. C. Valenti, and D. Torrieri, "Robust iterative noncoherent reception of coded FSK over block fading channels," *IEEE Trans. Wireless Commun.*, vol. 6, pp. 3142 - 3147, Sep. 2007.
- [18] J. G. Proakis and M. Salehi, *Digital Communications*, 5<sup>th</sup> Ed. New York: McGraw-Hill, 2008.
- [19] D. Torrieri, E. Ustunel, H. M. Kwon, S. Min, and D. H. Kang, "Iterative CDMA receiver with EM channel estimation and turbo decoding," in *Proc. IEEE MILCOM*, Washington D.C., pp. 1 - 6, Oct. 2006.
- [20] D. Torrieri, A. Mathur, A. Mukherjee, and H. M. Kwon, "Iterative LDPC CDMA receiver under time-varying interference," in *Proc. 65th IEEE Veh. Tech. Conf.*, Dublin, Ireland, pp. 1986 - 1989, Apr. 2007.
- [21] D. Torrieri, A. Mukherjee and H. M. Kwon, "Iterative EM channel estimation for DS-CDMA receiver using LDPC codes with M-ary modulation," in *Proc. IEEE MILCOM*, Orlando, FL, pp. 1 - 6, Oct. 2007.
- [22] X. Wautelet, C. Herzet, A. Dejonghe, J. Louveaux, and L. Vandendorpe, "Comparison of EM-based algorithms for MIMO channel estimation," *IEEE Trans. Commun.*, vol. 55, no. 1, pp. 216 - 226, Jan. 2007.
- [23] J. Choi, "An EM-based iterative receiver for MIMO-OFDM under interference-limited environments," *IEEE Trans. Wireless Commun.*, vol. 6, no. 11, pp. 3994 - 4003, Nov. 2007.
- [24] I. N. Psaromiligkos, S. N. Batalama, and M. J. Medley, "Rapid combined synchronization/demodulation structures for DS-CDMA systems - Part I: algorithmic developments," *IEEE Trans. Commun.*, vol. 51, no. 6, pp. 983 - 994, June 2003.

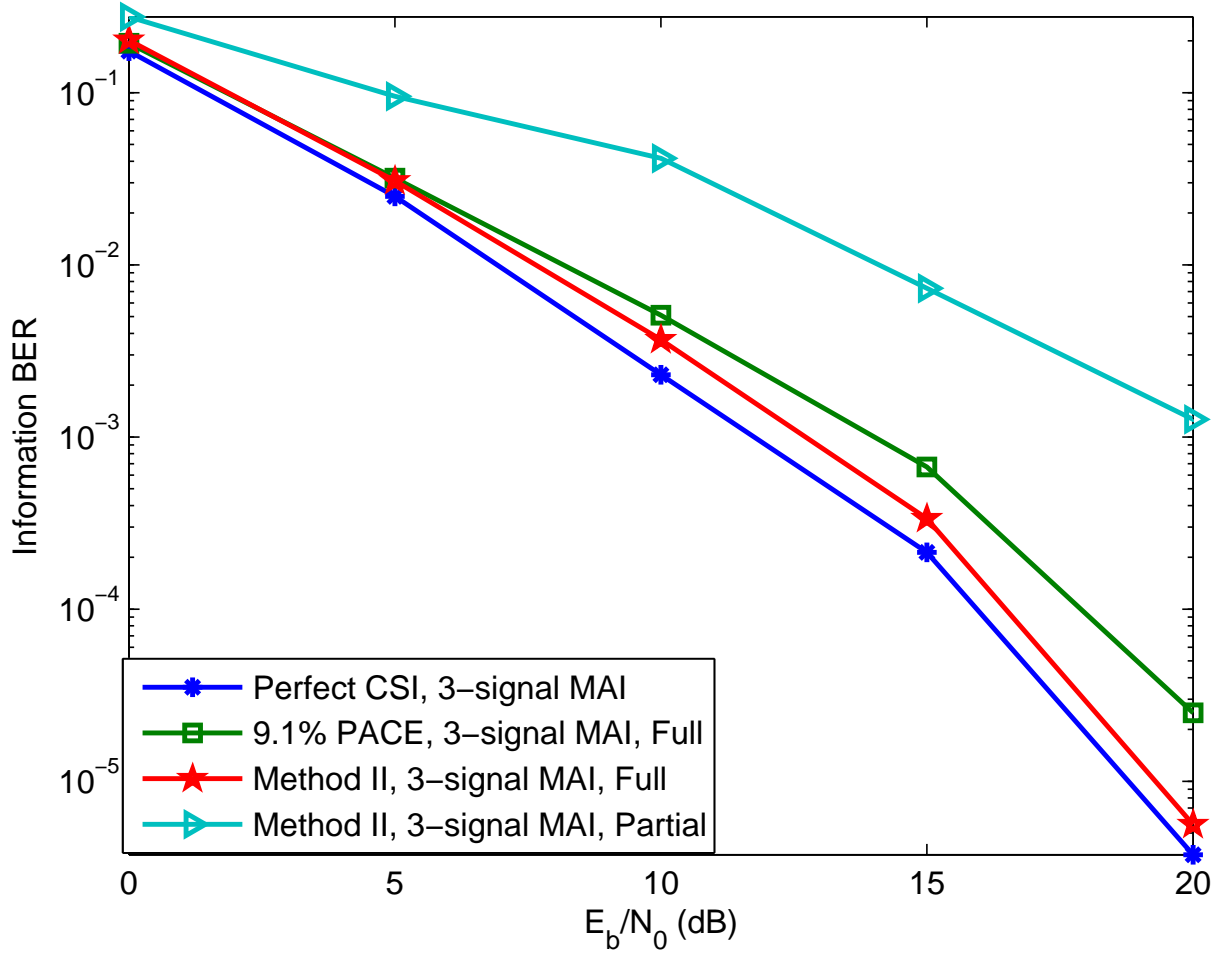


Fig. 10. BER versus  $E_b/N_0$  for IRA-coded iterative RAKE receiver with three resolvable multipath components and three fingers.

- [25] I. N. Psaromiligkos and S. N. Batalama, "Rapid combined synchronization/demodulation structures for DS-CDMA systems - Part II: finite data-record performance analysis," *IEEE Trans. Commun.*, vol. 51, no. 7, pp. 1162 - 1172, July 2003.
- [26] M. C. Necker and G. L. Stüber, "Totally blind APP channel estimation for mobile OFDM systems," *IEEE Trans. Wireless Commun.*, vol. 3, no. 5, pp. 1514 - 1525, Sep. 2004.
- [27] G. N. Karystinos and D. A. Pados, "Supervised phase correction of blind space-time DS-CDMA channel estimates," *IEEE Trans. Commun.*, vol. 55, no. 3, pp. 584 - 592, Mar. 2007.
- [28] M. Yang, W. E. Ryan, and Y. Li, "Design of efficiently encodable moderate-length high-rate irregular LDPC codes," *IEEE Trans. Commun.*, vol. 52, no. 4, pp. 564 - 571, Apr. 2004.
- [29] F. Peng, M. Yang, and W. Ryan, "Simplified eIRA code design and performance analysis for correlated Rayleigh fading channels," *IEEE Trans. Wireless Commun.*, vol. 5, no. 4, pp. 720 - 725, Apr. 2006.
- [30] T. Richardson, M. A. Shokrohalli, and R. Urbanke, "Design of capacity approaching irregular low density parity check codes," *IEEE Trans. Inf. Theory*, vol. 47, no. 2, pp. 619 - 637, Feb. 2001.
- [31] D. Torrieri, *Principles of Spread-Spectrum Communication Systems*. New York: Springer, 2005.
- [32] M. C. Valenti and S. Cheng, "Iterative demodulation and decoding of turbo coded M-ary noncoherent orthogonal modulation," *IEEE J. Selected Areas Commun.*, vol. 23, no. 9, pp. 1739 - 1747, Sep. 2005.
- [33] W. Oh and K. Cheun, "Iterative decoding and channel parameter estimation algorithms for repeat-accumulate codes," *IEEE Trans. Commun.*, vol. 53, no. 10, pp. 1597 - 1602, Oct. 2005.